Decreased Uptake of Iodinated Branched Fatty Acid Analog Indicates Metabolic Alterations in Ischemic Myocardium

Nagara Tamaki, Eiji Tadamura, Masahide Kawamoto, Yasuhiro Magata, Yoshiharu Yonekura, Yasuhisa Fujibayashi, Ryuji Nohara, Shigetake Sasayama and Junji Konishi

Department of Nuclear Medicine, Third Division, Department of Internal Medicine, Kyoto University Faculty of Medicine, Kyoto, Japan

We previously reported that uptake of ^{123}I-labeled 15-iodophenyl 3-methyl pentadecanoic acid (BMIPP) was lower than that of thallium in ischemic myocardium. Such discordant findings between BMIPP and thallium were compared with those of PET using ^{18}F-deoxyglucose (FDG) and ^{11}C-acetate to assess metabolic alterations in such segment. **Methods:** Sixteen patients with coronary artery disease underwent both BMIPP SPECT and PET. Relative FDG uptake (% FDG uptake) and the clearance rate constant (% Kmono) of ^{11}C-acetate from the myocardium were calculated as markers of glucose and oxidative metabolism, respectively. **Results:** Relative FDG uptake of the myocardial segments with reduced BMIPP uptake and normal thallium uptake (discordant segments) was similar (85.3 ± 10.3) to that of the normal segments (86.5 ± 11.7) but higher than that of segments with reduced uptake of both BMIPP and thallium (67.5 ± 19.9). Similarly, the discordant segments showed a higher % Kmono value (77.8 ± 13.1 versus 70.0 ± 19.1) and FDG-to-perfusion ratio (1.15 ± 0.08 versus 1.01 ± 0.22) than in the concordantly reduced segments. **Conclusion:** BMIPP uptake appears to provide metabolic information independent of thallium uptake. Combined imaging of BMIPP and thallium may potentially identify ischemic but viable myocardium.

Key Words: positron emission tomography; iodine-123-BMIPP; carbon-11-acetate; fluorine-18-FDG; coronary artery disease

J Nucl Med 1995; 36:1974–1980

Noninvasive assessment of myocardial metabolism using PET has played an important role in the evaluation and management of patients with coronary artery disease (CAD) (*1–3*). Since nonesterified fatty acids are the primary sources of energy for well-oxygenated myocardium in the fasting state, a variety of studies have focused on evaluating fatty acid metabolism using ^{11}C-palmitate (*4,5*). On the other hand, glucose is a major energy source for ischemic myocardium. Thus, PET [^{18}F]fluorodeoxyglucose (FDG), a marker of exogenous glucose utilization, has been used to detect ischemia and differentiate ischemic but viable myocardium from irreversible myocardial necrosis (*6–8*).

Because of the limited availability of PET, however, only a selected number of institutions with PET cameras and cyclotrons can study myocardial energy metabolism in vivo. Recently, a variety of ^{123}I-labeled fatty acid compounds have been introduced to probe myocardial energy metabolism in vivo using routine clinical nuclear medicine techniques (*9–16*). We previously reported the clinical value of ^{123}I-labeled 15-iodophenyl 3-methyl pentadecanoic acid (BMIPP) in patients with myocardial infarction (*17*). Little is known, however, about the uptake and retention mechanisms of this tracer (*18,19*). To clarify the uptake mechanism of BMIPP, its uptake was compared with PET findings using FDG and ^{11}C acetate.

METHODS

Patients

Consecutive patients with prior myocardial infarction or unstable angina who were referred from March 1993 to February 1994 for PET studies, to assess myocardial perfusion and metabolism, were included in this study. Each patient underwent BMIPP and thallium SPECT studies within 2 wk of the PET studies. We excluded patients who could not undergo either BMIPP or thallium studies at rest, those who did not undergo the ^{11}C-acetate PET study and those who received revascularization between these radionuclide studies. Thus, 16 patients were finally enrolled in this study. Fourteen had a history of acute myocardial infarction at least 1 mo previously and the other two had unstable angina. There were 3 women and 13 men, aged from 43 to 83 yr (mean 62 yr). Five patients had noninsulin-dependent diabetes mellitus. All but one patient, who had renal failure, underwent coronary angiography. Six patients had single-vessel disease, five had two-vessel disease and four had three-vessel disease. Left ventricular ejection fraction ranged from 35% to 65%, with a mean value of 47%. Twelve patients showed regional asynergy on contrast ventriculography. Each patient gave a written informed consent; the study protocol was approved by the Kyoto University Clinical Study Committee.

Received May 2, 1994; revision accepted Sept. 13, 1994.

For correspondence or reprints contact: Nagara Tamaki, MD, Department of Nuclear Medicine, Hokkaido University School of Medicine, Kita 15, Nishi 7, Sapporo 060, Japan.

BMIPP Preparation

BMIPP was prepared and supplied by Nihon Medi-Physics Co., Ltd. It contained 111 MBq (3 mCi) ^{123}I-labeled 15-(paraiodophenyl)-3-(R,S)-methyl pentadecanoic acid (0.6 mg) dissolved in 10.5 mg urso-deoxycholic acid (*17*).

BMIPP and Thallium Imaging

SPECT was performed 30 min after administration of 111 MBq (3 mCi) BMIPP at rest in a fasting state for at least 3 hr (*17*). SPECT images were obtained using a rotating gamma camera equipped with a low-energy, general-purpose collimator. A total of 32 views were obtained over 180° from the right anterior oblique to the left posterior oblique positions, taking 30 sec/per view (*17,20*).

Thallium SPECT imaging was performed on a separate day within 1 wk of the BMIPP SPECT study. Following administration of 100 MBq (2.7 mCi) thallium at rest, SPECT images were obtained 15 min later in a similar fashion as for the BMIPP study.

PET

The PET study was performed using a whole-body PET camera, which provides 15 slices at 7-mm intervals simultaneously. The scanner had an effective resolution of 9 mm and an axial resolution of 6 mm FWHM after reconstruction. Each patient was positioned under the camera with the use of an ultrasound technique (*21,22*). A transmission scan was obtained for 20 min using a ^{68}Ge/^{68}Ga source to correct for photon attenuation (*22*).

Approximately 185 MBq (5 mCi) FDG were administered at rest 40–60 min after a 75-g oral glucose load. Static images were obtained 60 min later for 15 min. Following reconstruction of 15 transverse tomograms, oblique tomograms parallel to the long- and short-axis of the left ventricle were also reformatted for comparison with the SPECT images.

On a different day, serial PET imaging was performed at rest following administration of 370 MBq (10 mCi) ^{11}C-acetate, acquiring 20 frames of 60 sec each for 20 min to assess oxidative metabolism.

Data Analysis

The left ventricular myocardium was divided into 17 segments and BMIPP and thallium uptake was scored by two experienced observers using a four-point grading system (3 = normal, 2 = mildly reduced, 1 = moderately reduced and 0 = absent) (*17*). The BMIPP uptake score was compared with the thallium score of the corresponding segment. When the BMIPP score was equal to the thallium score, the segments were considered to be concordant. Segments were defined as discordant when the BMIPP score was lower than the thallium score. No segment showed a BMIPP score greater than the thallium score.

In the analysis of ^{11}C-acetate PET images, time-activity curves of the corresponding 17 segments were generated from serial PET images after correction of deadtime, physical decay and cross-contamination (*22–24*). From these time-activity curves, the peak activity was determined as a marker of myocardial perfusion (*25*). In addition, the clearance rate constant (Kmono) of each segment was calculated by monoexponential fitting as a marker of oxidative metabolism (*22*).

In the analysis of FDG-PET images, FDG uptake was measured as 100% in the normal area to obtain the normalized FDG uptake (percentage of FDG uptake). Similarly, data for myocardial perfusion, Kmono value, BMIPP uptake and thallium uptake were normalized (%). Furthermore, the percent FDG uptake was divided by the percent perfusion to calculate the FDG-to-perfusion ratio to assess glucose-perfusion mismatch.

Statistical Analysis

Data were presented as mean ± s.d. Comparison of myocardial perfusion and metabolism was performed by unpaired Student's t-test (between two groups) or analysis of variance test (among three groups). Significant differences were considered to be present when the p value was less than 0.05.

RESULTS

Three patients without regional asynergy on contrast ventriculography had normal thallium and BMIPP scans. On the other hand, 12 patients with regional asynergy had reduced BMIPP uptake in at least one myocardial segment.

BMIPP and Thallium Findings

Of the total 272 segments, 146 segments showed normal distribution on both BMIPP and thallium scans (Group 1), 12 segments showed a decrease in BMIPP uptake with normal thallium uptake (Group 2), and 114 showed abnormal uptake on both BMIPP and thallium scans (Group 3). For Group III, 30 segments (26%) had a lower BMIPP than thallium score (discordant BMIPP uptake, Group 3a) (Fig. 1), whereas the remaining 84 segments had identical BMIPP and thallium scores (concordant BMIPP uptake, Group 3b) (Fig. 2).

PET

The semiquantitative PET data for each group are summarized in Table 1. The percent myocardial perfusion rate was significantly lower in Groups 2 (70.2 ± 8.2) and 3 (67.3 ± 18.3) than in Group 1 (86.5 ± 9.6) (both $p < 0.05$). On the other hand, the percent FDG uptake in Group 2 (85.3 ± 10.3) was similar to that in Group 1 (83.8 ± 11.7) and was higher in both groups than that in Group 3 (67.5 ± 19.9) (both $p < 0.05$). Therefore, the FDG-to-perfusion ratio was significantly higher in Group 2 (1.15 ± 0.08) than in Group 1 (0.98 ± 0.16) or Group 3 (1.01 ± 0.22) (both $p < 0.05$). In addition, the percent Kmono in Group 2 (77.8 ± 13.1) was similar to that in Group 1 (83.1 ± 11.6) and was higher in both groups than that in Group 3 (70.0 ± 19.1) (both $p < 0.05$).

When the segments in Group III were further divided into those with discordant BMIPP uptake (Group 3a) and those with concordant BMIPP uptake (Group 3b), the percent myocardial perfusion rate was similar in both groups (Table 2). The percent FDG uptake, however, was significantly higher in Group 3a (73.5 ± 16.8) than in Group 3b (65.3 ± 20.5) ($p < 0.05$). Therefore, the FDG-to-perfusion ratio was higher in Group 3a than in Group 3b (1.08 ± 0.18 versus 0.99 ± 0.23; $p < 0.05$). On the other hand, the Kmono did not differ between the two groups (72.5 ± 15.5 versus 69.0 ± 20.2; p = ns).

When BMIPP uptake was semiquantitativey calculated as a percentage of the peak activity, the percent BMIPP uptake was highly correlated with the percent thallium uptake ($r = 0.97$, Fig. 3). Thirty-five segments (13%), however, showed a percent BMIPP uptake 10% or more below the percent thallium uptake. On the contrary, only eight segments showed percent BMIPP uptake 10% or more

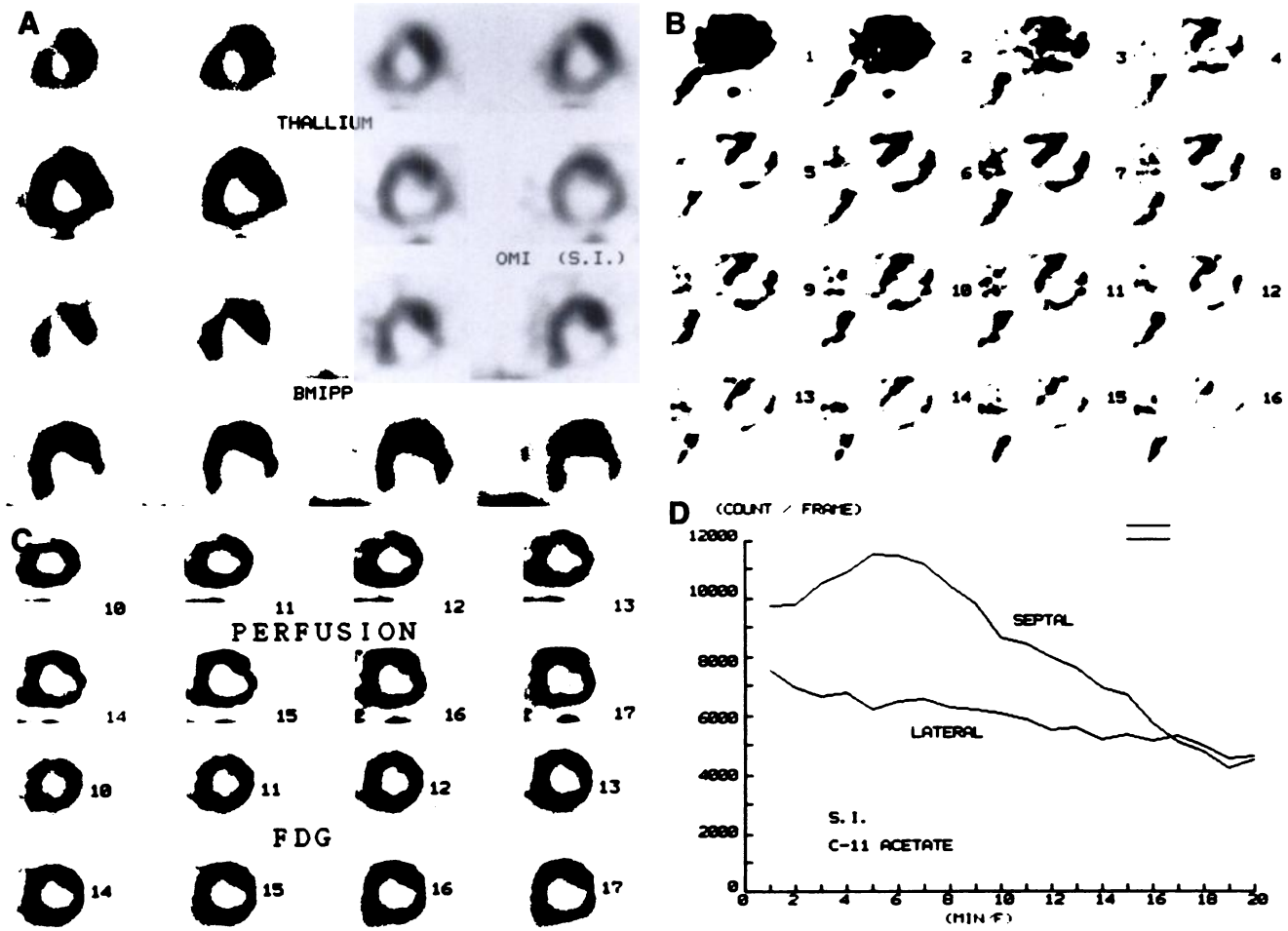

FIGURE 1. (A) Series of short-axis slices of ^{201}Tl (top) and BMIPP images (bottom) show hypoperfusion with further decrease in BMIPP distribution (discordant decrease) in the posterolateral regions in a 65-yr-old man with inferior wall myocardial infarction. (B) Series of short-axis slices of perfusion and FDG images show similar hypoperfusion with relatively preserved FDG uptake (glucose-perfusion mismatch) in the posterolateral region. (C) Serial dynamic PET images after administration of ^{11}C-acetate show decreased tracer uptake and delayed clearance in the apical and posterolateral regions. (D) Time-activity curves of the septal and posterolateral regions show decreased uptake and delayed tracer clearance in the posterolateral region, indicating reduced oxidative metabolism.

above the percent thallium uptake. All but one segment showed perfusion above 70% on the thallium scans. The percent BMIPP uptake also showed significant correlation with percent FDG uptake (r = 0.54) and percent Kmono (r = 0.50) (Fig. 4). Again, the percent BMIPP uptake was lower than the percent FDG uptake and Kmono values.

DISCUSSION

These results support our previous findings that reduced BMIPP uptake, compared with that of thallium (discordant BMIPP uptake), was often seen in patients with CAD. Areas with discordant BMIPP uptake were associated with glucose-perfusion mismatch on PET studies. In addition, oxidative metabolism in these segments were better preserved than that of the concordant segments, indicating that such segments may represent ischemic but viable myocardium.

Mechanisms of BMIPP Uptake

BMIPP is trapped in the endogenous lipid pool without further metabolism by beta oxidation after its distribution in the myocardium according to myocardial blood flow (*18,19*). Because of rapid clearance of the blood activity and long tracer retention in the myocardium, an excellent image of the ventricular myocardium is obtained, particularly with SPECT (*17*). Tracer distribution in the myocardium may be influenced by regional perfusion, fatty acid uptake and the turnover rate of the endogenous lipid pool. Our previous experimental study suggested a close relation of BMIPP uptake to the ATP content in the myocardium (*18,19*). Although BMIPP distribution seems to be similar to thallium distribution, striking differences in the distribution of these tracers have been reported in occlusion-reperfusion models (*26,27*) and cardiomyopathic hamsters (*28*), as well as in the clinical setting (*17,29,30*), indicating that BMIPP may provide metabolic information on the myocardium independent from that on myocardial perfusion.

Although the present study indicated that the BMIPP uptake correlated with thallium perfusion (Fig. 3), discordant BMIPP uptake less than thallium uptake was occa-

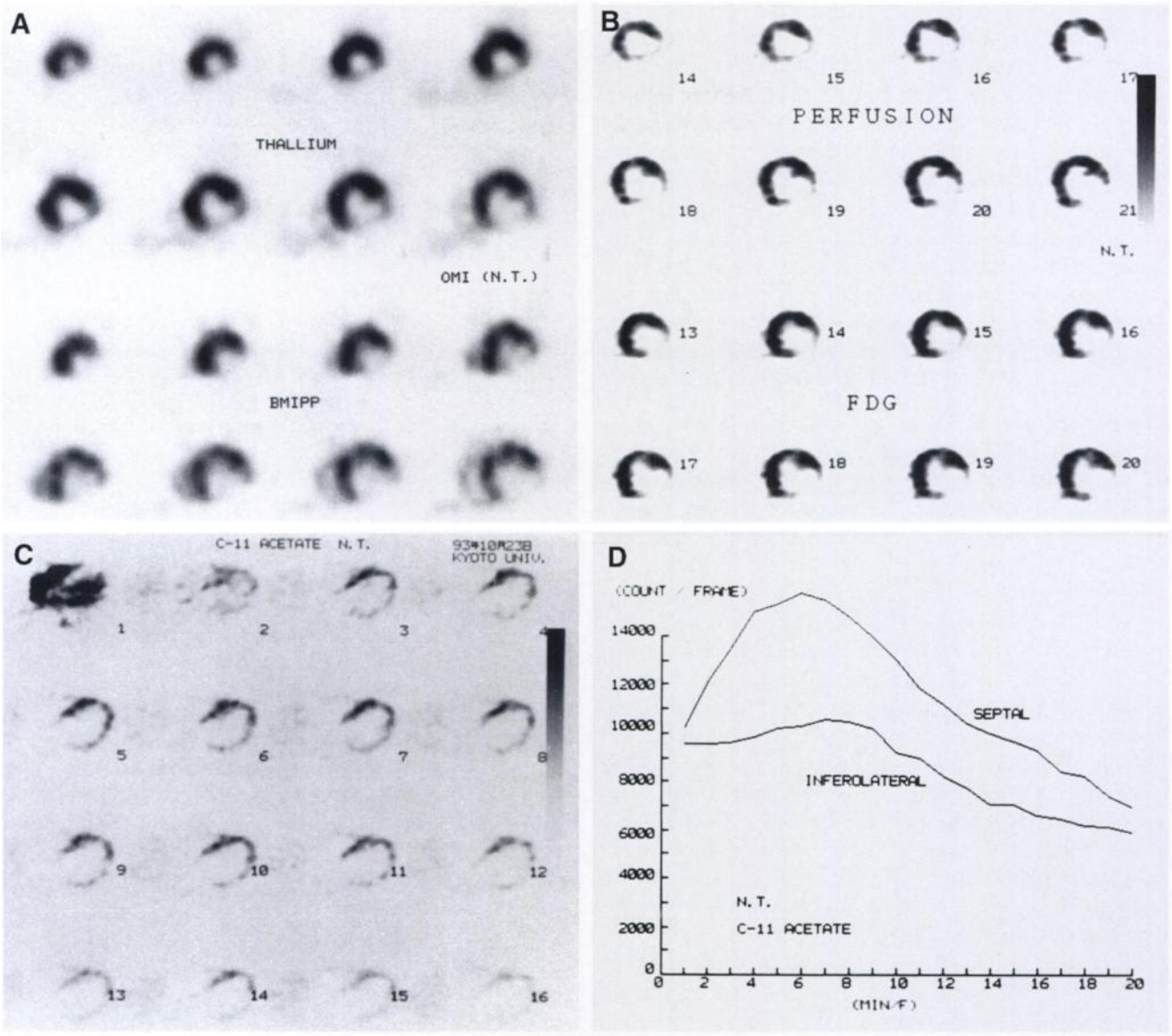

FIGURE 2. (A) Series of short-axis slices of ^{201}Tl (top) and BMIPP images (bottom) show a perfusion defect with concordant decrease in BMIPP distribution in the posterolateral region in a 76-yr-old man with inferior wall myocardial infarction. (B) Series of short-axis slices of perfusion and FDG images show similar decrease in perfusion and FDG uptake (matched defect) in the posterolateral region. (C) Serial dynamic PET images after administration of ^{11}C-acetate show decreased tracer uptake in the posterolateral region with delayed clearance. (D) Time-activity curves of the septal and posterolateral regions show decreased uptake and delayed tracer clearance in the posterolateral region, indicating reduced oxidative metabolism.

TABLE 1
Perfusion and Metabolism in Each Group

Group no.	No.	BMIPP	Tl	Perfusion (%)	FDG (%)	FDG/Perfusion	Kmono (%)
1	146	Normal	Normal	86.5 ± 9.6	83.8 ± 11.7	0.98 ± 0.16	83.1 ± 11.6
2	12	Reduced	Normal	70.0 ± 8.2*	85.3 ± 10.3	1.15 ± 0.08*‡	77.8 ± 13.1
3	114	Reduced	Reduced	67.3 ± 18.3*	67.5 ± 19.9*†	1.01 ± 0.22	70.0 ± 19.1*†

*$p < 0.05$ vs. Group 1; †$p < 0.05$ vs. Group 2; ‡$p < 0.05$ vs. Group 3.

sionally observed. Approximately, a quarter of the hypoperfused segments showed such discordance. In addition, among 158 segments with normal thallium distribution, 12 segments (8%) showed less BMIPP than thallium uptake. On the other hand, quantitative analysis indicated only a few segments showing higher BMIPP uptake than thallium distribution. Most of them were normoperfused segments. Such reverse discordance may be the result from the difference in photon attenuation between the tracers. These data were in agreement with our previous results in a study of patients with myocardial infarction (*17*). In addition, our previous report had a high reproducibility in the visual scoring of BMIPP and thallium uptake. The interobserver agreement was 87% for BMIPP and 91% for thallium (*17*).

Comparison with PET

To clarify BMIPP's uptake mechanism, a precise comparison of BMIPP uptake with the PET findings is required. PET is an excellent technique for probing myocardial energy metabolism in vivo using [^{18}F] FDG and ^{11}C-acetate as markers of exogenous glucose utilization and oxidative metabolism, respectively (*3–5,6–8*). In comparison with ^{11}C-palmitate, a radiolabeled free fatty acid (*4,5*), in our previous studies, BMIPP uptake had good correlation in its early uptake but not its early clearance rate, indicating that BMIPP uptake may reflect fatty acid retention rather than beta oxidation (*31*). In addition, discordant BMIPP uptake was associated with an increase in FDG uptake in the fasting state and redistribution on thallium stress scans, suggesting that the discordant BMIPP segments represented ischemic and jeopardized myocardium (*32*). Although the FDG study was performed after glucose loading (*33,34*), our present findings may support previous data that discordant segments represent ischemic myocardium on the basis of the glucose-perfusion mismatch. In particular, the segments with normal thallium uptake but reduced BMIPP uptake, which was occasionally observed in our patient studies, showed glucose-perfusion mismatch, indicating that some metabolic alteration has occurred. Although thallium uptake was within the normal range, the actual perfusion may have been slightly reduced compared to that of normal segments. The global scoring (four-point grading) of thallium may not differentiate subtle differences in perfusion. In addition, myocardial fatty acid utilization may possibly be suppressed with the reciprocal increase in glucose metabolism. When the segments with abnormal thallium perfusion were selected for analysis

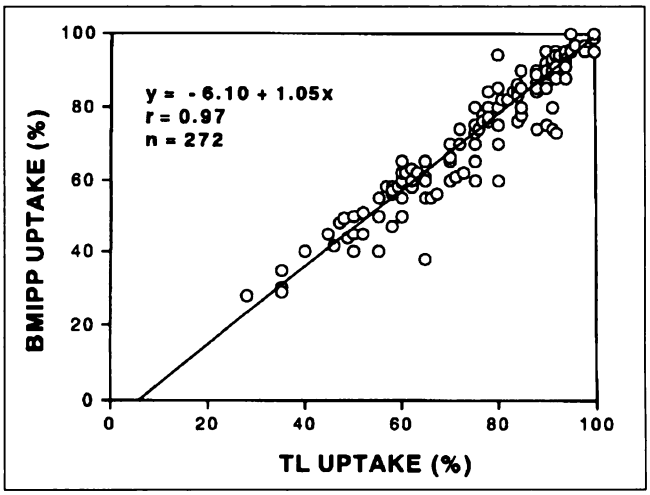

FIGURE 3. Correlation between percent BMIPP and ^{201}Tl uptake.

(Group 3), the segments with discordant BMIPP uptake also showed higher FDG-to-perfusion ratios than those with concordant BMIPP uptake, indicating that discordant BMIPP segments may represent ischemic but viable myocardium.

On the other hand, oxidative metabolism did not differ between Groups 3a and 3b. Two potential reasons are considered. The areas of discordant BMIPP uptake may represent severely ischemic myocardium mainly associated with anaerobic glucose metabolism. Alternatively, the percent Kmono value in Group 3a was higher than that in Group 3b, although the differences were not statistically significant. Thus, a larger patient study may indicate statistically significant differences between the two groups, suggesting that areas of discordant BMIPP uptake less than thallium may represent relatively preserved oxidative metabolism compared to the areas of concordant decrease both in BMIPP and thallium uptake.

In ischemic myocardium, fatty acid oxidation is suppressed and glucose becomes a major energy source (*35*). On the other hand, regional myocardial perfusion may persist to a certain extent to maintain energy metabolism without membrane damage. The percent BMIPP uptake was lower than the percent thallium uptake (Fig. 3). Similarly, the percent BMIPP uptake was lower than the percent FDG uptake or percent Kmono (Fig. 4). These data may support the idea that the BMIPP uptake is considered

TABLE 2
Perfusion and Metabolism in Group 3

Group no.	No.	Score	Perfusion (%)	FDG (%)	FDG/Perfusion	Kmono (%)
3a	30	BMIPP<Tl	68.4 ± 16.0	73.5 ± 16.8	1.08 ± 0.18	72.5 ± 15.5
3b	84	BMIPP=Tl	66.7 ± 19.0	65.3 ± 20.5*	0.99 ± 0.23*	69.0 ± 20.2

*$p < 0.05$ vs. Group 3a.

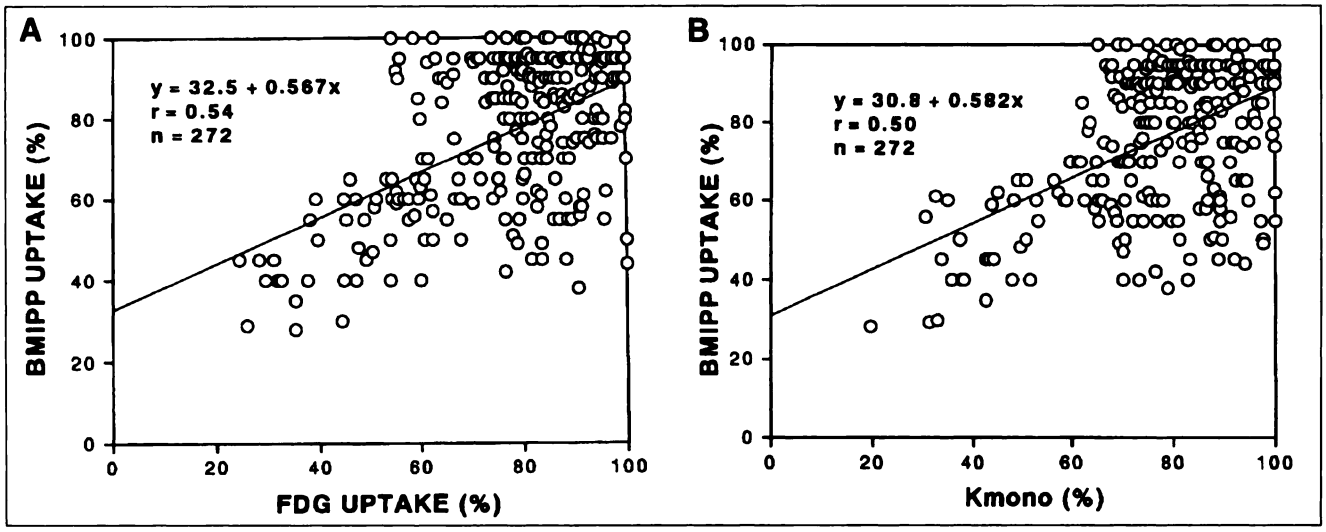

FIGURE 4. Correlation of (A) percentage BMIPP with FDG uptake and (B) percent Kmono.

to be a most sensitive marker of metabolic alterations in ischemic myocardium.

We hypothesized that discordant BMIPP uptake may reflect increased glucose utilization (*32*). The present study revealed that the areas with discordant BMIPP uptake were most likely to show glucose-perfusion mismatch (PET ischemia). On the contrary, a concordant decrease in both BMIPP and thallium may reflect a matched reduction in perfusion and glucose utilization (PET scar) (*6,7*).

Myocardial clearance of ^{11}C-acetate has been proven to be an excellent marker of oxidative metabolism in vivo using dynamic PET (*23,24*). In ischemic myocardium, oxidative metabolism may be suppressed but may still be relatively maintained compared to necrotic myocardium. Gropler et al. (*36*) reported that assessment of oxidative metabolism by PET and ^{11}C-acetate was useful for evaluating myocardial viability. Ischemic myocardium with preserved oxidative metabolism may represent reversible ischemic myocardium, which may improve regional function after revascularization. In areas of severe ischemia, however, blood flow may be too low to maintain either glucose or oxidative metabolism, resulting in myocardial necrosis (*36,37*).

These data indicate that combined imaging using BMIPP and thallium may provide valuable information about myocardial viability as an area of metabolic alterations. Further studies using combined SPECT imaging before and after revascularization are required to confirm our hypothesis.

Potential Limitations

One of the major limitations of this study was the comparison of SPECT images without attenuation correction and PET images that were corrected for photon attenuation. To minimize this limitation, BMIPP and thallium uptake were scored for each myocardial segment. Although an excellent correlation was observed between BMIPP and thallium uptake (Fig. 3), only a moderate correlation was obtained between BMIPP uptake and the PET studies (Fig. 4), probably due to the differences in photon attenuation.

Second, although the patients were enrolled consecutively, there was some bias to the patient selection, because patients who could not undergo both studies were excluded. Therefore, the number of patients in this study was rather limited.

It is controversial whether FDG-PET study should be performed under fasting or glucose loading conditions (*33,34,37*). Since FDG accumulates in the normal myocardium only during glucose loading, a glucose loading study is considered to be valuable for assessing tissue viability, whereas a fasting FDG-PET study seems to be useful for identifying ischemic myocardium (*34*). In this study, glucose loading was used since relative FDG uptake can be measured as 100% in the normal areas for comparison with other metabolic parameters.

CONCLUSION

We found that BMIPP often showed lower uptake than thallium in patients with CAD. Discordant segments also showed glucose-perfusion mismatch and preserved oxidative metabolism on PET images, indicating that they were ischemic but viable myocardium. These areas may represent jeopardized myocardium which requires revascularization therapy to improve regional function and prevent future cardiac events (*38,39*). Therefore, BMIPP may provide metabolic information that is independent of thallium uptake; this information may be useful in identifying ischemic but viable myocardium.

ACKNOWLEDGMENTS

The authors thank Tatsuhiko Hada, MD, Kazumi Okuda, MD and Shinji Ono, MD for assistance with the PET studies and Satoshi Sasayama, PhD, Toru Fujita, RT and the cyclotron staff for technical assistance. We also thank Nihon Medi-Physics for supplying the BMIPP.

Supported in part by a grant-in-aid for General Scientific Research from the Ministry of Education, Science, and Culture, Tokyo, Japan.

REFERENCES

1. Schelbert HR, Henze E, Phelps ME. Emission tomography of the heart. *Semin Nucl Med* 1980;10:355–373.
2. Bergmann SR, Fox KAA, Geltman EM, Sobel BE. Positron emission tomography of the heart. *Prog Cardiovasc Dis* 1985;28:165–194.
3. Schwaiger M, Hicks R. The clinical roles of metabolic imaging of the heart by positron emission tomography. *J Nucl Med* 1991;32:565–578.
4. Schon HR, Schelbert HR, Robinson G, et al. Carbon-11-labeled palmitic acid for the noninvasive evaluation of regional myocardial fatty acid metabolism with positron computed tomography. I. Kinetics of C-11 palmitic acid in normal myocardium. *Am Heart J* 1982;103:532–547.
5. Schelbert HR, Henze E, Keen R, et al. Carbon-11 palmitate for the noninvasive evaluation of regional myocardial fatty acid metabolism with positron computed tomography. IV. In vivo evaluation of acute demand-induced ischemia in dogs. *Am Heart J* 1983;106:736–750.
6. Marshall RC, Tillisch JH, Phelps ME, et al. Identification and differentiation of resting myocardial ischemia and infarction in man with positron computed tomography, ^{18}F-labeled fluorodeoxyglucose and ^{13}N ammonia. *Circulation* 1983;67:766–788.
7. Tillisch J, Brunken R, Marshall R, et al. Reversibility of cardiac wall-motion abnormalities predicted by positron tomography. *N Engl J Med* 1986;314: 884–888.
8. Tamaki N, Yonekura Y, Yamashita K, et al. Positron emission tomography using fluorine-18 deoxyglucose in evaluation of coronary artery bypass grafting. *Am J Cardiol* 1989;64:860–865.
9. Feinendegen LE, Vyska K, Freundlieb X, et al. Noninvasive analysis of metabolic reactions in body tissue: the case of myocardial fatty acids. *Eur J Nucl Med* 1981;6:191–200.
10. Kropp J, Lkungu J, Kirchhoff PG, et al. Single-photon emission tomography imaging of myocardial oxidative metabolism with 15-(p-(I-123) iodophenyl) pentadecanoic acid in patients with coronary artery disease and aorta-coronary bypass grafting surgery. *Eur J Nucl Med* 1991;18:467–474.
11. Murray G, Schad N, Ladd W, et al. Metabolic cardiac imaging in severe coronary artery disease: assessment of viability with iodine-123-iodophenyl pentadencanoic acid and multicrystal gama camera and correlation with biopsy. *J Nucl Med* 1992;33:1269–1277.
12. Herich MM, Vester E, Lohe von der E, et al. The comparison of 2-F-18-2-deoxyglucose and 15-(ortho-I-123-phenyl) pentadecanoic acid uptake in persistent defects on thallium-201 tomography in myocardial infarction. *J Nucl Med* 1991;32:1352–1357.
13. Reske SN. Iodine-123-phenyl pentadecanoic acid as a tracer of cardiac free fatty acid metabolism: experimental and clinical results. *Eur Heart J* 1985;6: 39–47.
14. Machulla HJ, Marsmann M, Dutschka K. Biochemical concept and synthesis of a radioiodinated phenylfatty acid for in vivo metabolic studies of the myocardium. *Eur J Nucl Med* 1980;5:171–173.
15. Knapp FF Jr, Ambrose KR, Goodman MM. New radioiodinated methyl-branched fatty acids for cardiac studies. *Eur J Nucl Med* 1986;12:S39–S44.
16. Ambrose KR, Owen BA, Goodman MM, Knapp FF Jr. Evaluation of the metabolism in rat heart of two new radioiodinated 3-methyl-branched fatty acid myocardial imaging agents. *Eur J Nucl Med* 1987;12:486–491.
17. Tamaki N, Kawamoto M, Yonekura Y, et al. Regional metabolic abnormality in relation to perfusion and wall motion in patients with myocardial infarction: assessment with emission tomography using an iodonated branched fatty acid. *J Nucl Med* 1992;33:659–667.
18. Fujibayashi Y, Yonekura Y, Takemura Y, et al. Myocardial accumulation of iodinated beta-methyl-branched fatty acid analogue, iodine-125-15-(p-iodophenyl)-3-(R,S) methyl pentadecanoic acid (BMIPP), in relation to ATP content. *J Nucl Med* 1990;31:1818–1822.
19. Fujibayashi Y, Som P, Yonekura Y, et al. Myocardial accumulation of iodinated beta-methyl-branched fatty acid analogue, iodine-125-15-(p-iodophenyl)-3-(R,S) methyl pentadecanoic acid (BMIPP), and correlation to ATP concentration II. Studies in salt-induced hypertensive rats. *Nucl Med Biol* 1992;2:62–66.
20. Tamaki N, Yonekura Y, Mukai T, et al. Stress thallium-201 transaxial emission computed tomography; quantitative versus qualitative analysis for evaluation of coronary artery disease. *J Am Coll Cardiol* 1984;4:1213–1221.
21. Tamaki N, Ohtani H, Yamashita K, et al. Metabolic activity in the areas of new fill-in after thallium-201 reinjection: comparison with positron emission tomography using fluorine-18-deoxyglucose. *J Nucl Med* 1991;32:673–678.
22. Tamaki N, Magata Y, Takahashi N, et al. Oxidative metabolism in the myocardium in normal subjects during dobutamine infusion. *Eur J Nucl Med* 1993;20:231–237.
23. Brown M, Marshall DR, Sobel BE, Bergmann SR. Delineation of myocardial utilization with carbon-11-labeled acetate. *Circulation* 1987;76:687–696.
24. Buxton DB, Nienaber CA, Luxen A, et al. Noninvasive quantitation of regional myocardial oxygen consumption in vivo with 1-^{11}C-acetate and dynamic positron emission tomography. *Circulation* 1989;79:134–142.
25. Gropler RJ, Siegel BA, Geltman EM. Myocardial uptake of carbon-11-acetate as an indirect estimate of regional myocardial blood flow. *J Nucl Med* 1991;32:245–251.
26. Nishimura T, Sago M, Kihara K. Fatty acid myocardial imaging using ^{123}I-β-methyl-iodophenyl pentadecanoic acid (BMIPP): comparison of myocardial perfusion and fatty acid utilization in canine myocardial infarction (occlusion and reperfusion model). *Eur J Nucl Med* 1989;15:341–345.
27. Miller DD, Gill JB, Elmaleh D, Arez T, Boucher CA, Strauss HW. Fatty acid analogue accumulation: a marker of myocite viability in ischemic-reperfused myocardium. *Circ Res* 1988;63:681–692.
28. Kurata C, Kobayashi A, Yamazaki N. Dual-tracer autoradiographic study with thallium-201 and radioiodinated fatty acid in cardiomyopathic hamsters. *J Nucl Med* 1989;30:80–87.
29. Saito T, Yasuda T, Gold HK, et al. Differentiation of regional perfusion and fatty acid uptake in zones of myocardial injury. *Nucl Med Commun* 1991;12: 663–675.
30. Kurata C, Taniguchi T, Aoshima S, et al. Myocardial emission computed tomography with iodine-123-labeled beta-methyl-branched fatty acid in patients with hypertrophic cardiomyopathy. *J Nucl Med* 1992;33:6–13.
31. Tamaki N, Kawamoto M, Yonekura Y, et al. Assessment of fatty acid metabolism using I-123 branched fatty acid: comparison with positron emission tomography. *Ann Nucl Med* 1993;7:S-II-41–47.
32. Kawamoto M, Tamaki N, Yonekura Y, et al. Combined study with I-123 fatty acid and thallium-201 to assess ischemic myocardium: comparison with thallium redistribution and glucose metabolism. *Ann Nucl Med* 1994;8:47–54.
33. Schelbert HR. Euglycemic-hyperinsulinemic clamp and oral glucose load in stimulating myocardial glucose utilization during positron emission tomography. *J Nucl Med* 1992;33:1263–1266.
34. Tamaki N, Yonekura Y, Konishi J. Myocardial FDG-PET studies with the fasting, oral glucose loading or insulin clamp methods. *J Nucl Med* 1992;33: 1263–1268.
35. Neely JR, Rovetto MJ, Oran JF. Myocardial utilization of carbohydrate and lipids. *Prog Cardiovasc Dis* 1972;15:289–301.
36. Gropler RJ, Geltman EM, Sampathkumaran K, et al. Comparison of carbon-11-acetate with fluorine-18-fluorodeoxyglucose for delineating viable myocardium by positron emission tomography. *J Am Coll Cardiol* 1993;22:1587–1597.
37. Takahashi N, Tamaki N, Kawamoto M, et al. Glucose metabolism in relation to perfusion in patients with ischemic heart disease under fasting and glucose loading conditions. *Eur J Nucl Med* 1994;21:292–296.
38. Eitzman D, Al-Aouar Z, Kanter HL, et al. Clinical outcome of patients with advanced coronary artery disease after viability studies with positron emission tomography. *J Am Coll Cardiol* 1992;20:559–565.
39. Tamaki N, Kawamoto M, Takahashi N, et al. Prognostic value of an increase in fluorine-18 deoxyglucose uptake in patients with myocardial infarction: comparison with stress thallium imaging. *J Am Coll Cardiol* 1993;22:1621–1627.